Available online at www.sciencedirect.com
ScienceDirect
Ceramics International 36 (2010) 47–54
CERAMICS INTERNATIONAL
www.elsevier.com/locate/ceramint

The effect of ceramic nanoparticles on tribological properties of alumina sol–gel thin coatings

Ireneusz Piwoński *, Katarzyna Soliwoda

University of Lodz, Department of Chemical Technology and Environmental Protection, Pomorska 163, 90-236 Łódź, Poland

Received 14 May 2009; received in revised form 30 May 2009; accepted 26 June 2009
Available online 16 July 2009

Abstract

Thin alumina coatings containing zirconia or alumina nanoparticles having diameter of ~20–30 nm were deposited by the sol–gel dip-coating process on silicon wafers. The mass content of nanoparticles in the alumina coating was fixed at 15% in relation to the theoretical mass of alumina matrix resulted from the amount of the applied precursor. Atomic force microscopy (AFM) was used to image the surface topography of as-made coatings and find out the wear level after frictional tests. Tribological tests were performed with the use of a microtribometer operating in the load range of 30–100 mN. It was found that the presence of α-alumina (corundum) or zirconia nanoparticles enhances the tribological performance of alumina layers annealed at 100 °C by decreasing the average wear rate by 20% and 63% for zirconia and corundum nanoparticles, respectively. No wear was observed for samples containing both types of nanoparticles annealed at 500 °C.

Keywords: B. Nanocomposites; B. Optical microscopy; C. Wear resistance; D. Al_2O_3; D. ZrO_2; Sol–gel; Nanoparticles; Coefficient of friction; AFM; Microtribometer

1. Introduction

Alumina thin coatings have been intensively investigated because of their unique properties and practical applications. Due to the high mechanical and chemical resistance, high hardness and corrosion resistance alumina coatings are broadly applied as protective layers [1–5], in optical [6,7], electronic [8,9] and automobile industry up to aerospace applications [10].

High performance alumina coatings exhibiting high wear resistance were reported by Hübert et al. [3,5]. The preparation of alumina layers performed with the use of aluminium-tri-sec-butoxide as alumina precursor in 2-methoxyethanol was reported in [5]. Layers deposited by dip-coating were annealed at 100, 500 and subsequently at 900–1100 °C in argon or in vacuum. In order to get thicker layers the precursor solution was aged for 1 week and than the deposition and drying procedures were repeated several times. It was found that such layers exhibit high adhesion to the metal substrate due to the formation of chemical bonds at the metal/layer interphase and reveal high abrasive wear resistance particularly in the case of samples annealed at 1000 °C due to the formation of hard α-Al_2O_3 (corundum).

Generally alumina coatings are deposited using numerous methods like chemical vapor deposition CVD [11], physical vapor deposition PVD [12], combustion flame pyrolysis [13], reactive bipolar pulsed magnetron sputtering [14], and sol–gel [3,5,9,15–17]. CVD and PVD are suitable especially for alumina deposition as protective coatings for cuttings tools [18].

However, the sol–gel method seems to be superior to other techniques since being simple, cheap, low-temperature and not requiring vacuum. Moreover, this method enables preparation of high purity and highly homogenous materials containing one or more constituents in the form of mono- or multilayers. It was also found that thin layers prepared by the sol–gel approach exhibit better adhesion to the substrate as compared to CVD and PVD techniques.

Thin alumina layers may be prepared by the sol–gel using as precursors organic alkoxides [3,5,9,15,16] or inorganic salts [19,20]. One of the first reports about preparation of alumina layers was presented by Yoldas and Bulent [21]. Transparent alumina sol was obtained by hydrolysis of isopropoxy

* Corresponding author. Tel.: +48 42 635 58 33; fax: +48 42 635 58 32.
E-mail address: irek@uni.lodz.pl (I. Piwoński).

0272-8842/$36.00
doi:10.1016/j.ceramint.2009.06.024

aluminium in water. Acetic acid was used as peptization agent in molar ratios water:alkoxide:acid 100:1:0.5. The resulting mixture after heating in 80 °C in water/alkoxide environment had consistencies of slurry, which transformed to transparent sol after 8 h.

Vazquez et al. [17] used aluminium-tri-sec-butoxide—$Al(OBu^s)_3$ as precursor in the synthesis of alumina coatings. Initially the precursor was mixed with anhydrous ethanol. Next, water was added in order to initiate gentle gelation of the mixture during 1 h. Final product was dried in air flow and calcined at 1000 °C. XRD and FT-IR measurements revealed that coatings annealed at 1000 °C were crystalline (γ and small fraction of α form) while coatings annealed at 1000–1100 °C contained only α-Al_2O_3.

Özer et al. [16] investigated optical and corrosion properties of alumina coatings prepared by sol–gel spin-coating on stainless steel. The reaction was carried out in the presence of isopropanol as a solvent and aluminium-tri-sec-butoxide—$Al(OBu^s)_3$ as alumina precursor, acetyloacetone as chelating agent and nitric acid as catalyst. Coatings were annealed at 400 °C. Resulted layers were characterized by XRD, XPS, FT-IR, optical spectroscopy and by microhardness tests. XRD measurements revealed that samples were amporphous. It was found that alumina layers improved microhardness and corrosion resistance of the stainless-steel substrate.

Although there are many methods of preparation of high hardness alumina coatings, the main problem which limits their use in technological applications is the low resistance of alumina for cracking under stress. In spite of its hardness, alumina is very brittle. However, it is known that the mechanical properties of the materials may be enhanced if the grain size of its constituents reaches the nanometrical range. Mechanical properties of nanocomposites are at the centre of interest of numerous studies [10,22–26] including alumina coatings. Alumina is also doped with nanoparticles creating nanocomposites in order to improve its mechanical properties. As a result materials having opposite properties (i.e. high hardness and high bending strength) may be synthesized. Moreover, the presence of a nanodisperse phase also improves the triblogical properties of the material.

Voevodin and Zabinski [10] reported an example of such nanocomposites consisting of 15–25 vol% of MoS_2 nanoparticles having diameter of 2–4 nm dispersed in the alumina matrix. Such nanocomposite exhibits very low coefficient of friction ($\mu = 0.02$) and low wear. These properties are also preserved in extreme environmental conditions like high vacuum, low temperatures or in thermal shocks. Due to their properties such composites are excellent materials for space applications.

Measurements performed by Niihara et al. [27] also confirm that even small amounts of SiC nanoparticles (5 vol%) enhances the antiwear properties of alumina and the bending resistance.

Yang et al. [28] investigated the influence of zirconia nanoparticles on the mechanical and microstructural properties of Ce-TZP/Al_2O_3 composites (TZP—tetragonal zirconia polycrystal). It was found that optimal properties i.e. the highest hardness and the maximum resistance for cracking exhibits the material containing 20% of nanoparticles (in relation to the matrix mass). At this concentration nanoparticles may be easily dispersed in the material filling in the dislocations and increasing the hardness and wear resistance. For higher content of the nanoparticles (more than 20%) their distribution in the material is not homogenous due to the formation of agglomerates. Therefore, the reduction of the antiwear properties of the material is observed.

The goal of this work was preparation the sol–gel alumina coatings containing corundum or zirconia nanoparticles and investigation of the effect of nanoparticles on the coefficient of friction (CoF) and wear. CoF was measured with the use of the microtribometer. Wear scare analysis was performed using optical microscopy and atomic force microscopy (AFM). The surface topography of the coatings containing nanoparticles was imaged with the use of AFM and compared with coatings prepared without nanoparticles.

2. Experimental

2.1. Materials and coating preparation

Aluminium-tri-sec-butoxide (Fluka Chemie GmbH, Sigma–Aldrich Chemika, Switzerland), Acetyloacetone–2,4-pentanodione (Ubichem, Eastleigh, Hampshire, UK), nanoparticles Al_2O_3 and ZrO_2 (AGH University of Science and Technology, Krakow, Poland), Ethanol (POCh, Gliwice, Poland), Isopropanol (POCh, Gliwice, Poland), Silicon wafers (Cemat Silicon S.A., Poland).

Pure alumina coatings and alumina nanocomposites coatings containing nanoparticles were prepared on silicon wafers Si(1 0 0) using a modified Özer's procedure [16]. Si wafers were thoroughly cleaned in dry ethanol prior to deposition. The general overview of the procedure is presented in Fig. 1.

In order to prepare purely alumina coatings, aluminium-tri-sec-butoxide $Al(O\text{-}C_4H_9)_3$ was added to isopropanol. Next,

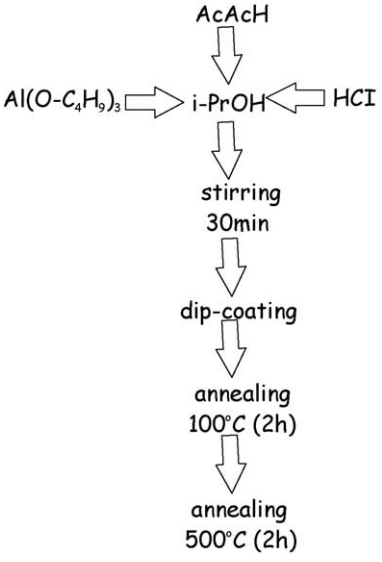

Fig. 1. Flow sheet of the preparation of the alumina coatings.

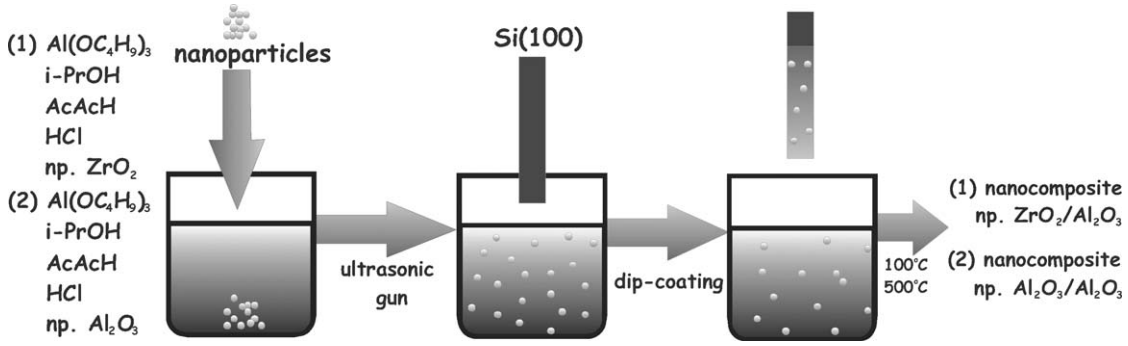

Fig. 2. Preparation procedure of the alumina-composite coatings.

acetyloacetone was added as chelating agent and 2 M HCl as a catalyst. The whole mixture was 30 min magnetically stirred. Resulted sol was deposited on silicon wafers using a computer controlled dip-coating procedure with immersion and withdrawal rates of 25 mm min^{-1}. After deposition, the coatings were annealed 2 h at 100 and 500 °C.

Nanocomposites were prepared by a similar procedure as described above. After 15 min mixing, the desired amount of nanoparticles was introduced to the sol and dispersed in ultrasonic bath for another 15 min using an ultrasonic gun (IKA Labortechnik U200S, US-200-14, 14 mm, 105 W cm^{-1}, amplitude 50 μm), keeping the same time of the alumina sol treatment. The amount of the nanoparticles was fixed at 15 wt.% of the theoretical mass of alumina matrix created in the sol–gel process. Nanocomposites were annealed 2 h at 100 and 500 °C. The preparation procedure of the sol–gel alumina coatings containing corundum or zirconia nanoparticles is presented in Fig. 2.

Detailed amounts of the compounds used in the preparation of alumina coatings and alumina-composite coatings are collected in Table 1.

2.2. AFM measurements

The surface topography was imaged with the use of commercial NT-MDT AFM equipped with a Smena head operating in air under ambient conditions in the tapping mode. Non-contact silicon cantilevers covered by silicon nitride was used (MikroMash, NSC35/Si_3N_4/AlBS) having spring constant $k = 14$ N m^{-1} and the resonance frequency $\nu = 260$ kHz. The typical scan area was fixed at 10 μm × 10 μm. Imaging of the wear scares formatted at normal load 60 mN was performed in similar conditions at larger scanning areas up to 100 μm × 100 μm.

Table 1
Detailed composition of the bath used in the preparation of alumina coatings.

Compound	M [g mol^{-1}]	n [mmol]	d [g cm^{-3}]	[cm^3]	m [g]
Al(O-C_4H_9)$_3$	246.33	0.005	0.960	1.249	1.20
i-PrOH	60.11	0.226	0.785	17.325	13.60
AcAcH	100.13	0.050	0.972	0.530	0.52
HCl	36.51	0.001	1.190	0.034	0.04
np.ZrO_2*	123.22	3.0×10^{-4}	–	–	0.037
np.Al_2O_3	101.96	3.6×10^{-4}	–	–	0.037

* np.: nanoparticles.

2.3. Tribological tests

Frictional measurements (CoF) were performed with the use of a microtribometer designed and constructed at the Department of Chemical Technology and Environmental Protection University of Lodz operating in the load range up to 100 mN. Coefficients of friction under technical dry friction conditions were recorded in ambient conditions with the following parameters:

Counterpart:	ZrO_2/Y_2O_3 ball Ø 5 mm
Velocity:	25 mm min^{-1}
Frictional distance:	10 mm
Normal load range:	30–100 mN
Normal load interval:	10 mN
Number of cycles:	8 (one cycle consisted of moving sample up and down at given normal load always on the new path)

Resulting coefficient of friction is an average value of the three independent measurements performed at the same environmental conditions in short time. The average error between measurements within one series did not exceed 5%.

2.4. Wear scare analysis using optical microscopy

Optical microscope at 24× (8 × 3) magnification designed for metallographic imaging was applied in the wear scare analysis of samples after frictional tests performed using the microtribometer. The analysis consisted of the measurement of the average width of all visible wear scares formatted in microtribological tests in eight cycles at normal loads 30–100 mN. The scare width was calculated as arithmetical average of the width measurements of the two scares at given normal loads originated from rising counterpart up and down at the sample surface.

3. Results and discussion

Fig. 3 presents the comparison of the AFM surface topography images of alumina coatings and nanocomposite alumina coatings containing 15% of ZrO_2 or Al_2O_3 nanoparticles annealed at 100 and 500 °C.

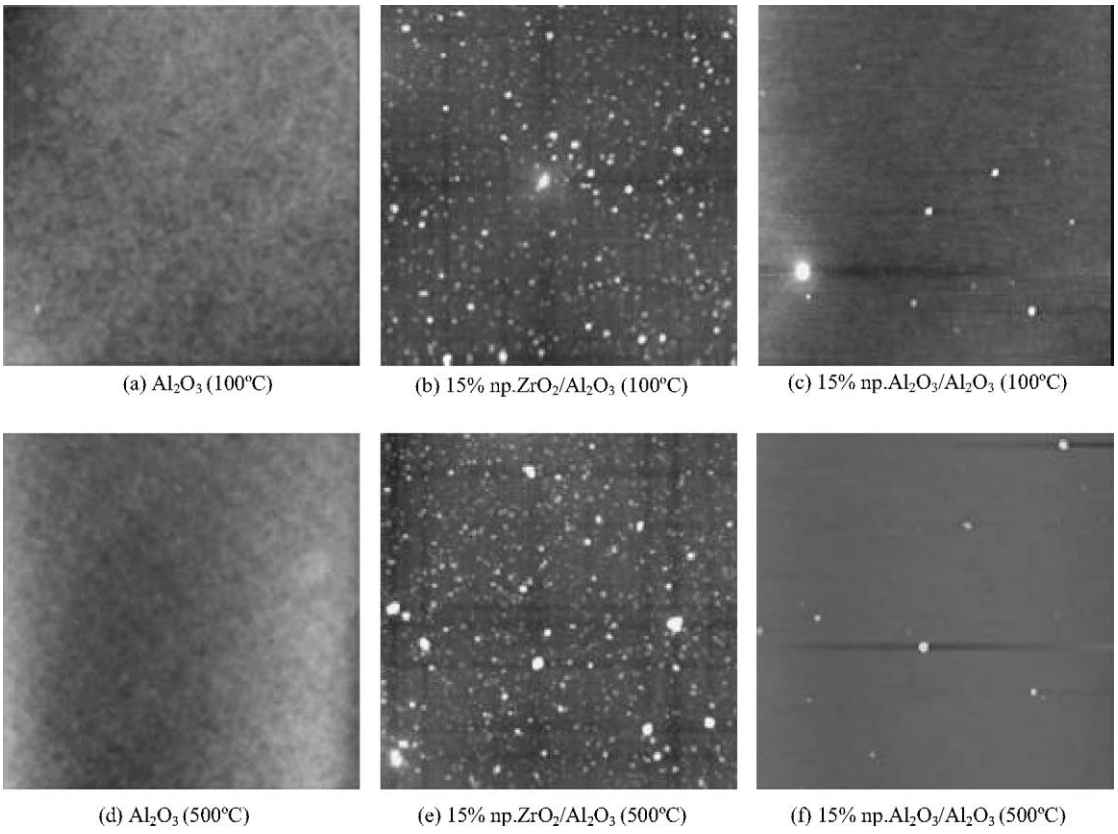

Fig. 3. AFM images (10 μm × 10 μm) of alumina coatings and composite alumina coatings containing 15% of ZrO_2 or Al_2O_3 nanoparticles annealed at 100 and 500 °C. (a) Al_2O_3 (100 °C). (b) 15% np.ZrO_2/Al_2O_3 (100 °C). (c) 15% np.Al_2O_3/Al_2O_3 (100 °C). (d) Al_2O_3 (500 °C). (e) 15% np.ZrO_2/Al_2O_3 (500 °C). (f) 15% np.Al_2O_3/Al_2O_3 (500 °C).

Alumina coatings after treatment at 100 and 500 °C are homogenous, smooth and do not exhibit any cracks over the large scan areas. The surface roughness oscillates at very low level for both samples i.e. $R_{a\text{-}100} = 0.44$ nm and $R_{a\text{-}500} = 0.41$ nm for samples treated at 100 and 500 °C, respectively.

Higher surface roughness is observed for nanocomposite alumina coatings containing zirconia nanoparticles, respectively: $R_{a\text{-}100} = 1.77$ nm and $R_{a\text{-}500} = 3.41$ nm. A large number of agglomerates having average size of 40 nm in the alumina coating containing zirconia nanoparticles is observed, however their distribution is homogeneous (Fig. 3b and e).

In the case of alumina coating containing corundum nanoparticles, the number of agglomerates is much smaller but the size of visible objects reaches 100 nm. Better dispersion of nanoparticles in the alumina matrix may be observed for corundum nanoparticles due to the fact that the dispersed nanophase and the matrix are built of the same material (Fig. 3c and f). As a consequence, the surface roughness is much lower than in the case of alumina coatings containing zirconia nanoparticles: $R_{a\text{-}100} = 0.67$ nm and $R_{a\text{-}500} = 0.77$ nm.

Microtribological measurements revealed high value of CoF ≈ 1 for all alumina materials annealed at 100 °C. Such value seems to be unusually high. However, the measurements were conducted at very low counterpart velocities (25 mm min^{-1}) and in dry friction conditions without any lubrication. Moreover, samples annealed at 100 °C are amorphous and relatively soft. These circumstances favor creation of strong adhesive interactions between the coating and zirconia counterpart. An increase of the temperature treatment up to 500 °C causes the drop of CoFs as compared to samples treated at 100 °C due to the formation of crystalline phase γ-Al_2O_3 exhibiting higher hardness [29]. The results of CoF measurements are collected in Fig. 4. In the case of nanocomposites containing 15% of zirconia nanoparticles in alumina treated at 500 °C an increase of the CoF was observed probably due to the high number of zirconia agglomerates

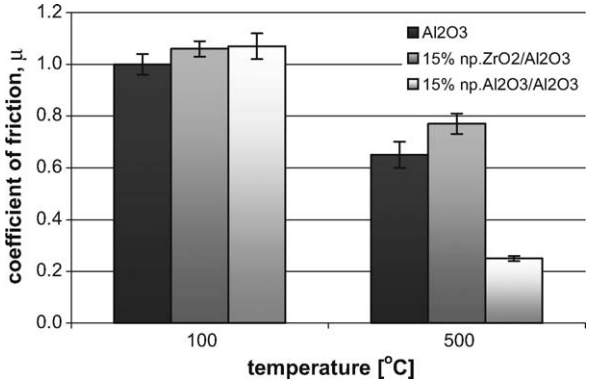

Fig. 4. Friction coefficients of alumina coatings and composite alumina coatings containing 15% of ZrO_2 or Al_2O_3 nanoparticles annealed at 100 and 500 °C.

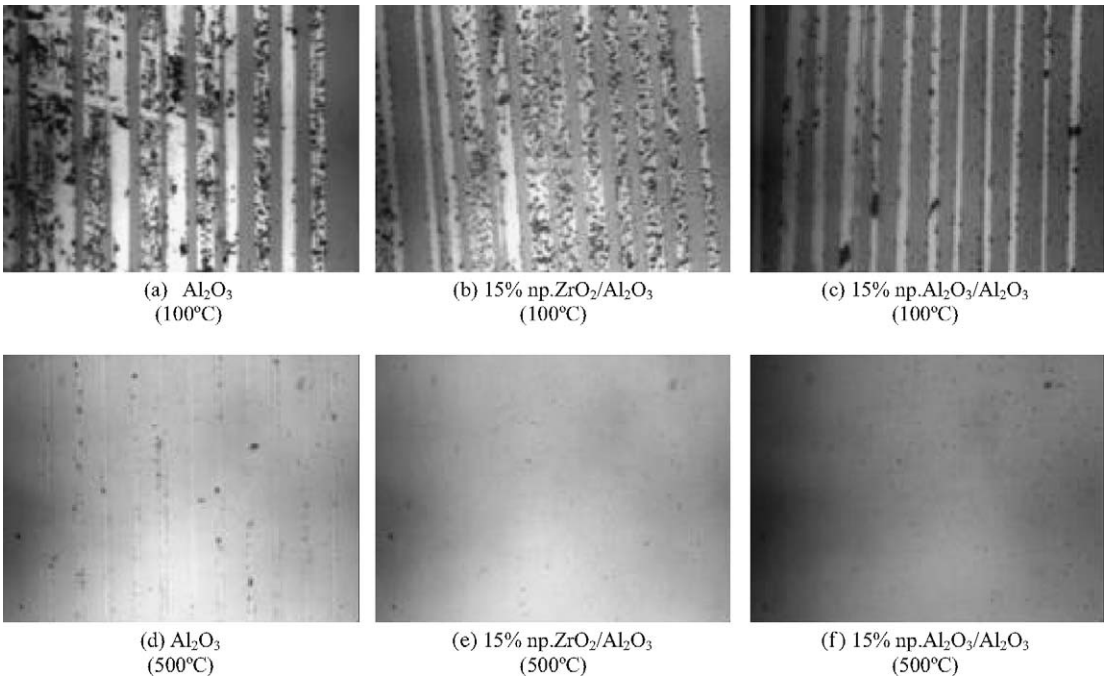

Fig. 5. Optical microscope images of the wear tracks after tribological tests of alumina coatings and composite alumina coatings containing 15% of ZrO_2 or Al_2O_3 nanoparticles annealed at 100 and 500 °C. (a) Al_2O_3 (100 °C). (b) 15% np.ZrO_2/Al_2O_3 (100 °C). (c) 15% np.Al_2O_3/Al_2O_3 (100 °C). (d) Al_2O_3 (500 °C). (e) 15% np.ZrO_2/Al_2O_3 (500 °C). (f) 15% np.Al_2O_3/Al_2O_3 (500 °C).

present in the alumina coatings and differences in surface roughness.

Better parameters are exhibited by system consisting of corundum nanoparticles in the alumina matrix where the drop of CoF is observed from 0.65 to 0.25 for purely alumina sample and nanocomposite, respectively (Fig. 4).

Contrarily to CoF measurements, much better effect of the presence of nanoparticles on the antiwear properties of alumina composite was observed. The addition of nanophase into the alumina matrix considerably enhances its antiwear properties as revealed by the optical microscope of the wear tracks after the tribological tests (Fig. 5). The dependence of the wear tracks width on applied normal loads (30–100 mN) at a given temperature for alumina and alumina nanocomposites is presented in Fig. 6a and b.

The width of the wear track was considerably narrower when the ZrO_2 or Al_2O_3 nanoparticles were present in the alumina coatings in the fixed amount of 15%. These changes refer to both temperatures of sample annealing i.e. 100 and 500 °C. In the case of the composite containing 15% of alumina nanoparticles in the alumina coating annealed at 100 °C the average wear track had 1/3 of the width of the initial wear tracks measured for purely alumina coating without nanoparticles annealed at the same temperature. As well, for alumina coating annealed at 100 °C the depth of the wear tracks was reduced from 60 nm for alumina to 10 nm for alumina containing 15% of zirconia nanoparticles (Fig. 7a). The analysis performed with the use of AFM technique clearly shows that in case of purely alumina coatings the wear tracks are very broad, and the material of the coating was removed completely during sliding

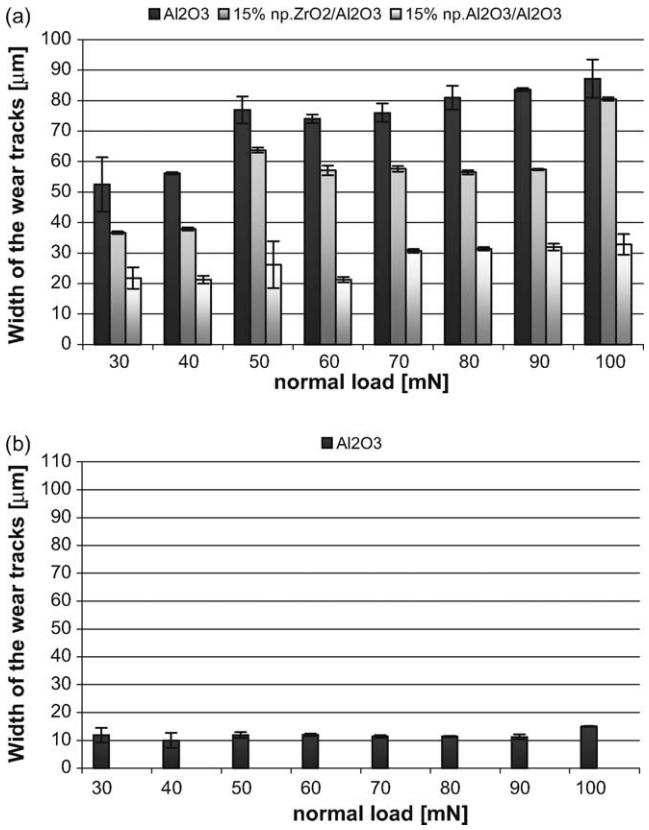

Fig. 6. (a) The wear tracks width for alumina and alumina coatings containing ZrO_2 or Al_2O_3 nanoparticles annealed at 100 °C. (b) The wear tracks width for alumina coatings annealed at 500 °C. No wear was observed for alumina coatings containing ZrO_2 or Al_2O_3 nanoparticles.

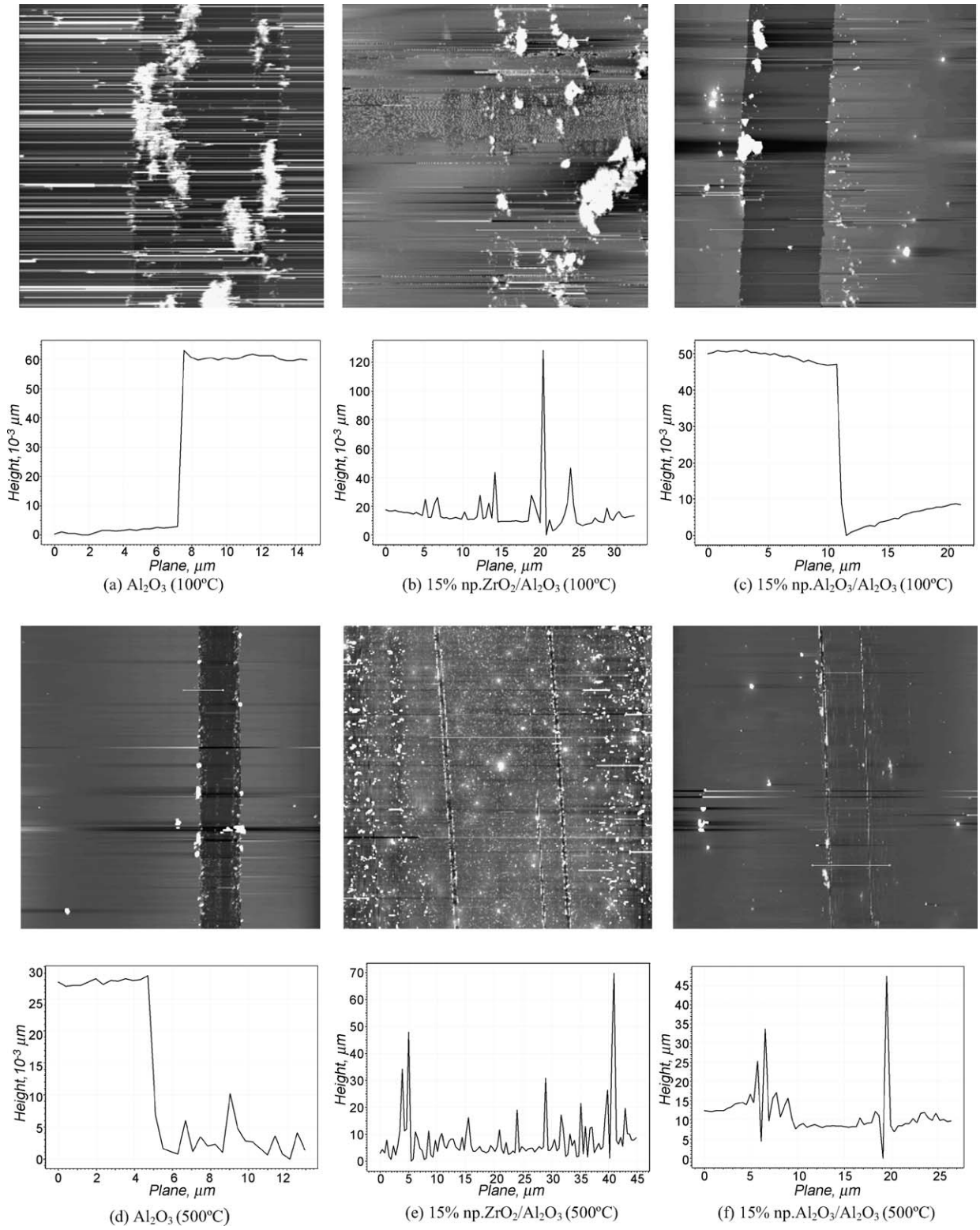

Fig. 7. AFM images (100 μm × 100 μm) and cross-sections of the wear tracks resulted in tribological tests at normal load of 60 mN. (a) Al_2O_3 (100 °C). (b) 15% np.ZrO_2/Al_2O_3 (100 °C). (c) 15% np.Al_2O_3/Al_2O_3 (100 °C). (d) Al_2O_3 (500 °C). (e) 15% np.ZrO_2/Al_2O_3 (500 °C). (f) 15% np.Al_2O_3/Al_2O_3 (500 °C).

of the counterbody. The wear tracks are narrower and the material of the coating is removed only partially for the nanocomposite.

The most pronounced changes were observed for coatings annealed at 500 °C due to the fact that the addition of nanoparticles enabled the preparation of a nanocomposite coating exhibiting no wear in the range of applied load 30–100 mN (Fig. 6). More detailed analysis of the wear tracks revealed that in the case of the alumina coatings annealed at 500 °C the wear track is broad and the depth of the wear track is

Table 2
The surface parameters and tribological characteristics of alumina and alumina-composite coatings.

	Al_2O_3	15% np.ZrO_2/Al_2O_3	15% np.Al_2O_3/Al_2O_3
100 °C			
R_a [nm]	0.44	1.77	0.67
μ	1.0 ± 0.04	1.06 ± 0.03	1.05 ± 0.05
d_{30} [μm]	52.5 ± 8.9	36.7 ± 0.4	21.8 ± 3.5
d_{40} [μm]	56.1 ± 0.4	37.9 ± 0.6	21.3 ± 1.3
d_{50} [μm]	76.9 ± 4.4	63.7 ± 0.8	26.1 ± 5.7
d_{60} [μm]	74.0 ± 1.4	57.1 ± 1.6	21.3 ± 0.9
d_{70} [μm]	76.0 ± 3.0	57.6 ± 0.9	30.7 ± 0.6
d_{80} [μm]	80.9 ± 3.9	56.5 ± 0.7	31.4 ± 0.5
d_{90} [μm]	83.6 ± 0.5	57.4 ± 0.2	32.0 ± 1.1
d_{100} [μm]	87.2 ± 6.3	80.5 ± 0.6	32.8 ± 3.4
Average wear for all normal loads [μm]	73.4 ± 12.6	55.9 ± 14.0	27.2 ± 5.1
Depth of the wear tracks [nm]	60	10	50
500 °C			
R_a [nm]	0.41	3.41	0.77
μ	0.65 ± 0.05	0.77 ± 0.06	0.25 ± 0.01
d_{30} [μm]	11.9 ± 2.6	0	0
d_{40} [μm]	10.0 ± 2.7	0	0
d_{50} [μm]	11.9 ± 1.0	0	0
d_{60} [μm]	12.0 ± 0.4	0	0
d_{70} [μm]	11.4 ± 0.5	0	0
d_{80} [μm]	11.4 ± 0.2	0	0
d_{90} [μm]	11.2 ± 0.9		0
d_{100} [μm]	15.0 ± 0.1	0	0
Average wear for all normal loads [μm]	11.9 ± 1.4	0	0
Depth of the wear tracks [nm]	25	0	10

R_a: rms surface roughness; μ: coefficient of friction; d_{30}: wear scares width at normal load of 30 mN.

25 nm. The addition of the corundum nanoparticles considerably reduces the wear track width, the material of the coating is removed only partially and the local average depth of the wear track is 10 nm (Fig. 7f). The best performance is exhibited by the nanocomposite consisting of 15% zirconia nanoparticles in the alumina coating. In the case of this nanocomposite no wear was observed but only minor cracks (Fig. 7e). The surface parameters and tribological characteristics of alumina and alumina-composite coatings are collected in Table 2.

4. Conclusions

Alumina and alumina-composite coatings containing nanoparticles were successfully prepared by the sol–gel dip-coating method. The AFM surface analysis exhibited various topographies indicating homogenous distribution of corundum nanoparticles in the alumina matrix. In the case of zirconia nanoparticles, agglomerate-like structures are visible at the composite surface; however their distribution remains still homogenous.

The presence of nanoparticles improved the tribological properties of the investigated materials. The antiwear properties were considerably enhanced by doping the alumina with nanoparticles. The best performance is exhibited by the sample doped with 15 wt.% of corundum and zirconia nanoparticles annealed at 500 °C. Synergistic effect of the temperature and the presence of nanoparticles is observed since at higher temperatures crystalline forms of alumina are formed.

Acknowledgements

Authors would like to direct special thanks to Dr Zbigniew Pędzich from AGH University of Science and Technology, Krakow-Poland for providing corundum and zirconia nanoparticles.

References

[1] H.M. Hawthorne, A. Neville, T. Troczynski, X. Hu, M. Thammachart, Y. Xie, J. Fu, Q. Yang, Characterization of chemically bonded composite sol–gel based alumina coatings on steel substrates, Surf. Coat. Technol. 176 (2004) 243–252.
[2] C.Z. Huang, J. Wang, X. Ai, Development of new ceramic cutting tools with alumina coated carbide powders, Int. J. Mach. Tools Manuf. 40 (2000) 823–832.
[3] T. Hübert, J. Schwarz, B. Oertel, Sol–gel alumina coatings on stainless steel for wear protection, J. Sol–Gel Sci. Technol. 38 (2006) 179–184.
[4] A.R. Phani, F.J. Gammel, T. Hack, Structural, mechanical and corrosion resistance properties of Al_2O_3–CeO_2 nanocomposites in silica matrix on Mg alloys by a sol–gel dip coating technique, Surf. Coat. Technol. 201 (2006) 3299–3306.
[5] T. Hübert, S. Svoboda, B. Oertel, Wear resistant alumina coatings produced by a sol–gel process, Surf. Coat. Technol. 201 (2006) 487–491.
[6] B. Chen, D. Yang, P.A. Charpentier, S. Nikumb, Optical and structural properties of pulsed laser deposited Ti:Al_2O_3 thin films, Sol. Energy Mater. Sol. Cells 92 (2008) 1025–1029.
[7] T. Ishizaka, Y. Kurokawa, T. Makino, Y. Segawa, Optical properties of rare earth ion (Nd^{3+}, Er^{3+} and Tb^{3+})-doped alumina films prepared by the sol–gel method, Opt. Mater. 15 (2001) 293–299.
[8] T. Olding, M. Sayer, D. Barrow, Ceramic sol–gel composite coatings for electrical insulation, Thin Solid Films 398/399 (2001) 581–586.

[9] K. Vanbesien, P. De Visschere, P.F. Smet, D. Poelman, Electrical properties of Al_2O_3 films for TFEL-devices made with sol–gel technology, Thin Solid Films 514 (2006) 323–328.
[10] A.A. Voevodin, J.S. Zabinski, Nanocomposite and nanostructured tribological materials for space applications, Compos. Sci. Technol. 65 (2005) 741–748.
[11] S. Ruppi, Deposition, microstructure and properties of texture-controlled CVD α-Al_2O_3 coatings, Int. J. Refract. Met. Hard Mater. 23 (2005) 306–316.
[12] A. Aryasomayajula, N.X. Randall, M.H. Gordon, D. Bhat, Tribological and mechanical properties of physical vapor deposited alpha alumina thin film coating, Thin Solid Films 517 (2008) 819–823.
[13] R. Kavitha, V. Jayaram, Deposition and characterization of alumina films produced by combustion flame pyrolysis, Surf. Coat. Technol. 201 (2006) 2491–2499.
[14] K. Bobzin, E. Lugscheider, M. Maes, C. Pińero, Relation of hardness and oxygen flow of Al_2O_3 coatings deposited by reactive bipolar pulsed magnetron sputtering, Thin Solid Films 494 (2006) 255–262.
[15] C. Jing, X. Zhao, Y. Zhang, Sol–gel fabrication of compact, crack-free alumina film, Mater. Res. Bull. 42 (2007) 600–608.
[16] N. Özer, J.P. Cronin, Y.J. Yao, A.P. Tomsia, Optical properties of sol–gel deposited Al_2O_3 films, Sol. Energy Mater. Sol. Cells 59 (1999) 355–366.
[17] A. Vazquez, T. Lopez, R. Gomez, Bokhimi, A. Morales, O. Novarot, X-ray diffraction, FTIR, and NMR characterization of sol–gel alumina doped with lanthanum and cerium, J. Solid State Chem. 128 (1997) 161–168.
[18] D.H. Kuo, B.Y. Cheung, R.J. Wu, Growth and properties of alumina films obtained by low-pressure metal–organic chemical vapor deposition, Thin Solid Films 35 (2001) 398–399.
[19] Q. Fu, C.B. Cao, H.S. Zhu, Preparation of alumina films from a new sol–gel route, Thin Solid Films 348 (1999) 99–102.
[20] W. Zhang, W. Liu, Q. Xue, Characterization and tribological investigation of Al_2O_3 and modified Al_2O_3 sol–gel films, Mater. Res. Bull. 36 (2001) 1903–1914.
[21] B.E. Yoldas, E. Bulent, Alumina sol preparation from alkoxides, Am. Ceram. Soc. Bull. 54 (1975) 289–290.
[22] J. Patscheider, T. Zehnder, M. Diserens, Structure–performance relations in nanocomposite coatings, Surf. Coat. Technol. 146/147 (2001) 201–208.
[23] A.A. Voevodin, J.S. Zabinski, C. Muratore, Recent advances in hard, tough, and low friction nanocomposite coatings, Tsinghua Sci. Technol. 10 (2005) 665–679.
[24] A.A. Voevodin, J.S. Zabinski, Supertough wear-resistant coatings with 'chameleon' surface adaptation, Thin Solid Films 370 (2000) 223–231.
[25] R. Hauert, J. Patscheider, From alloying to nanocomposites-improved performance of hard coatings, Adv. Eng. Mater. 2 (2000) 247–259.
[26] P. Holubaru, M. Jilek, M. Sima, Present and possible future applications of superhard nanocomposite coatings, Surf. Coat. Technol. 133/134 (2000) 145–151.
[27] K. Niihara, T. Koichi, S. Akihiro, New design concept of structural ceramics, ceramic nanocomposites, J. Ceram. Soc. Jpn. 99 (1991) 523–536.
[28] G. Yang, J. Li, G. Wang, M. Yashima, S. Min, Influences of ZrO_2 nanoparticles on the microstructure and mechanical behavior of Ce-TZP/Al_2O_3 nanocomposites, J. Mater. Sci. 40 (2005) 6087–6090.
[29] Y. Kobayashi, T. Ishizaka, Y. Kurokawa, Preparation of alumina films by the sol–gel method, J. Mater. Sci. 40 (2005) 263–283.